Article

Chinese Science Bulletin

Physical Chemistry

March 2012 Vol.57 No.9: 976–983
doi: 10.1007/s11434-011-4971-4

Electronic properties and stabilities of methoxy-substituted Lindqvist polyoxometalates $[Nb_2W_4O_{19}CH_3]^{3-}$ by DFT

CONG Sha[1], YAN LiKai[1,2*], SONG Ping[1], GUAN Wei[1], SU ZhongMin[1*] & SUN ChiaChung[2]

[1] *Institute of Functional Material Chemistry, Department of Chemistry, Northeast Normal University, Changchun 130024, China;*
[2] *State Key Laboratory of Theoretical and Computational Chemistry, Institute of Theoretical Chemistry, Jilin University, Changchun 130023, China*

Received June 9, 2011; accepted November 13, 2011; published online February 8, 2012

The electronic properties and stabilities of five $[Nb_2W_4O_{18}OCH_3]^{3-}$ isomers have been investigated using a density functional theory method. The results show that the isomer with the methoxy group occupying a bridging position between two tungsten atoms (two tungsten atoms in the plane that contains two niobium atoms) in the $[Nb_2W_4O_{18}OCH_3]^{3-}$ framework is the most stable isomer in acetonitrile. The stability of the one-electron-reduced isomers changes little. The most stable one-electron-reduced isomer has the methoxy group occupying a bridging position between niobium atoms in the $[Nb_2W_4O_{18}OCH_3]^{4-}$ framework. The M–O_b (M = Nb, W; b denotes bridging) bond lengths in anions in which the metal atoms are connected by a methoxy group are longer than those in $[Nb_2W_4O_{19}]^{4-}$. The highest occupied molecular orbitals (HOMO) in $[Nb_2W_4O_{19}]^{4-}$ mainly delocalize over the bridging oxygen atoms of two niobium atoms and two tungsten atoms located in the equatorial plane, and the bridging oxygen atoms on the axial surface. The lowest unoccupied molecular orbitals (LUMO) of $[Nb_2W_4O_{19}]^{4-}$ are mainly concentrated on the tungsten atoms and antibonding oxygen atoms. Methoxy substitution modifies the electronic properties of the $[Nb_2W_4O_{18}OCH_3]^{3-}$ isomers. The HOMOs in the five isomers formally delocalize over the bridging oxygen atoms, which are distant from the surface containing the methoxy group and four metal atoms. The LUMOs delocalize over the d-shells of the four metal atoms that are close to the methoxy group, and the p-orbitals of oxygen. One-electron reduction occurred at the tungsten atoms, not the niobium atoms.

polyoxometalates, Lindqvist structures, electronic properties, stability, DFT

Citation: Cong S, Yan L K, Song P, et al. Electronic properties and stabilities of methoxy-substituted Lindqvist polyoxometalates $[Nb_2W_4O_{19}CH_3]^{3-}$ by DFT. Chin Sci Bull, 2012, 57: 976–983, doi: 10.1007/s11434-011-4971-4

Polyoxometalates (POMs) are polynuclear complexes built primarily by edge and corner sharing of MO_6 octahedra; the resulting cages are usually approximately spherical [1–3]. Typical elements that form molecular (discrete) metal oxides are W^{VI}, Mo^{VI}, and V^{V} because their ionic radii and charges are suitable for combining with O^{2-} [4]. POMs have been known in 1826 by Berzelius, but it was not until a century later that Keggin reported the first POM structure. POMs have been subjected to a large number of studies because of their attractive electronic and molecular properties; these properties give rise to a variety of applications, for example, in catalysis [5], medicine [6,7], and materials science [8,9].

Lindqvist polyanions $[M_6O_{19}]^{n-}$ are an important class of POMs. Lindqvist structures are formed by the full range of 4d and 5d polyanion-forming metal ions (Nb^{V}, Ta^{V}, Mo^{VI}, and W^{VI}). The structures of these anions are all close to the O_h symmetry. In 1950, Lindqvist [10] reported the structures of $(NH_4)_6Mo_7O_{24}\cdot 4H_2O$ and $(NH_4)_4Mo_8O_{26}\cdot 5H_2O$. Tytko and co-workers [11] subsequently reported the structures of $[Nb_6O_{19}]^{8-}$, $[Ta_6O_{19}]^{8-}$, $[Mo_6O_{19}]^{2-}$, and $[W_6O_{19}]^{2-}$. Dabbabi and co-workers [12] reported the structure of $[Nb_2W_4O_{19}]^{4-}$. Spectral and electrochemical investigations showed that the two niobium atoms of the $[Nb_2W_4O_{19}]^{4-}$

*Corresponding authors (email: yanlk924@nenu.edu.cn; zmsu@nenu.edu.cn)

anion are in *cis* positions. $[Nb_2W_4O_{19}]^{4-}$ is known to be sufficiently basic to form stable organometallic derivatives and can therefore be reasonably expected to form stable covalent organic derivatives $[Nb_2W_4O_{19}R]^{3-}$, where R is an alkyl or silyl group. Poblet and co-workers [13] reported the relative basicity of the external oxygen sites in $[Nb_2W_4\text{-}O_{19}]^{4-}$; the results show that the oxygen bonded to two niobium atoms is the most basic center. Day et al. [14] synthesized $[Nb_2W_4O_{19}CH_3]^{3-}$ by different pathways. IR and NMR spectroscopic data show that the $[Nb_2W_4O_{19}CH_3]^{3-}$ anion forms a mixture of five species, with the methoxy group occupying a different doubly bridging site in each isomer. In addition, there are two chiral isomers among the five isomers. The physical and chemical properties of the five isomers drew our attention. Which is the most stable one? Which is the more stable of the two chiral isomers? How does the methoxy group modify the structural and electronic properties? Which atom is preferred as the electron acceptor when the $[Nb_2W_4O_{19}CH_3]^{3-}$ is reduced?

Thanks to the rapid development of density functional theory (DFT) [15] methods and computer technology, high-level calculations on large metal systems have recently been carried out. DFT calculations correctly described the redox properties of anions with transition-metal heteroatoms such as Co(II), Co(III), or Fe(III) [16,17]. Our group has investigated the electronic properties, stabilities, and nonlinear optical properties of POMs using DFT methods [18–22]. DFT has proved to be an important tool for understanding and rationalizing the properties of polyanions [23–30]. In this work, our main objective is to investigate the effects of methoxy groups on the electronic properties of POMs. DFT theoretical studies of the five $[Nb_2W_4O_{19}\text{-}CH_3]^{3-}$ isomers are presented. The stabilities and electronic properties of the $[Nb_2W_4O_{19}CH_3]^{3-}$ isomers are studied. We hope that the theoretical predictions will support and guide experimental studies. In particular, the stabilities of the systems we studied are very helpful in experiments to separate the five $[Nb_2W_4O_{19}CH_3]^{3-}$ isomers.

1 Computational details

Large systems with heavy metals that need to take both electron correlation and relativistic effects into account require much computational effort. DFT methods are a good alternative for studying heavy-metal complexes [31–33], and have been used successfully to calculate electronic properties, redox potentials, and even polarizabilities [34–38]. In this study, DFT calculations were carried out using the ADF2009.01 program [39–41]. The local density approximation characterized by the Vosko-Wilk-Nusair functional [42] parameterization is adopted as the correlation functional. Becke [43] and Perdew [44] gradient corrections were used for the exchange and correlation energy, respectively. The basis functions for describing the valence electrons of the atoms are Slater-type orbitals of triple-zeta plus polarization TZP quality; these have been used to investigate the properties of POMs [26,28,30,45]. The internal or core electrons (1s for oxygen, 1s for carbon, 1s–3d for niobium, 1s–4d for tungsten) were frozen and described by single Slater functions. We applied scalar relativistic corrections, and zero-order regular approximations [46–49], via the core potentials generated with the DIRAC [50] program. Spin-restricted calculations were performed on six ground-state structures, and for one-electron-reduced states, unrestricted open-shell calculations were performed. The value of the numerical integration parameter used to determine the precision of the numerical integrals was 6.0. All the structures discussed were optimized in the presence of a model solvent, accounted for with the conductor-like screening model [51,52]. To define the cavity surrounding the molecules, we used the solvent-excluding-surface method and fine tesserae. The ionic radii of the polyanion atoms, which were defined by the size of the solvent cavity where the target molecule remains, were chosen to be 1.26 Å for the niobium and tungsten atoms [53,54]. The radii for oxygen, carbon, and hydrogen are 1.52, 1.70, and 1.20 Å, respectively. The dielectric constant (ε) used in the computations was set to 37.5 to model the effects of acetonitrile, which was used in the experiments. In this work, we used the statistical average of orbital potentials, described by Schipper et al. [55], to calculate the excitation energies of the studied systems. Frequency calculations for the five $[Nb_2W_4O_{19}\text{-}CH_3]^{3-}$ isomers were performed and confirmed that the structures are minima at 298.15 K.

2 Results and discussion

2.1 Geometric structures

It is well known that the oxygen atoms in Lindqvist polyanions and their derivatives can be divided into three categories: terminal oxygen (O_t), bridging oxygen (O_b), and central oxygen (O_c) atoms. For the purposes of comparison, calculations were also performed for $[Nb_2W_4O_{19}]^{4-}$ (Figure 1, system A). Methylation of $[Nb_2W_4O_{19}]^{4-}$ yields five $[Nb_2W_4O_{19}CH_3]^{3-}$ anions containing methoxy groups in five possible doubly bridging sites in $[Nb_2W_4O_{19}]^{4-}$, i.e., systems B, C, D, E, and F (Figure 1). The surface including the two niobium atoms is called the equatorial plane and the surface that is perpendicular to the equatorial plane is referred to as the axial surface. Five kinds of O_b atoms are classified and shown in Figure 1.

The system geometries were optimized under C_{2v} symmetry for $[Nb_2W_4O_{19}]^{4-}$, C_s for F and B, and C_1 for C, D and E, respectively (Figure 1).

Some selected bond lengths are listed in Table 1. The bonds in $[Nb_2W_4O_{19}CH_3]^{3-}$ are different from those in $[Nb_2W_4O_{19}]^{4-}$. In $[Nb_2W_4O_{19}CH_3]^{3-}$, the bond lengths of M–O_b (M = Nb, W), in which the metal atoms are connected to

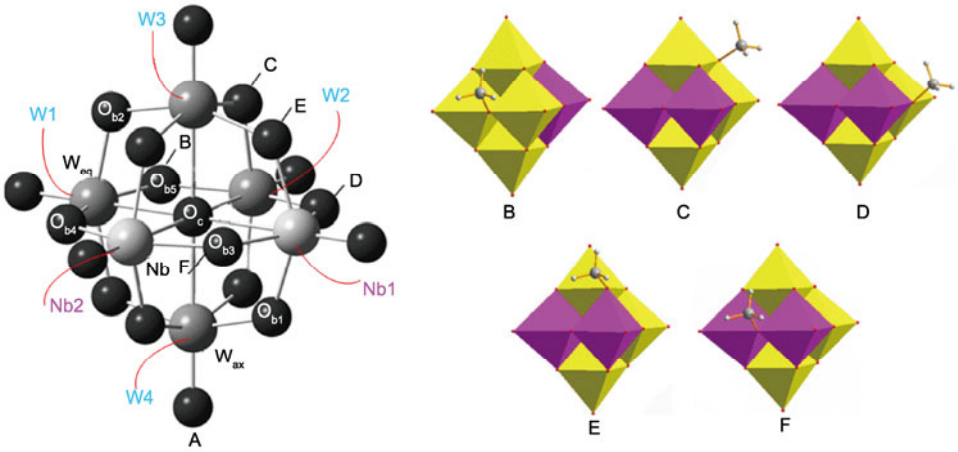

Figure 1 (Color online) Calculation models. A is a ball-and-stick view of $[Nb_2W_4O_{19}]^{4-}$. Dark-gray and gray spheres represent tungsten and niobium atoms, respectively; black spheres represent oxygen atoms. The polyhedra represent the five $[Nb_2W_4O_{19}CH_3]^{3-}$ isomers.

Table 1 Selected bond lengths (Å) of systems A to F

	A	B	C	D	E	F
Nb–O_c	2.444	2.544	2.431	2.433	2.446	2.434
Nb–O_{b1}	2.046	2.042	2.049	2.037	2.190*	2.031
Nb–O_{b3}	1.987	1.974	1.988	1.954	1.973	2.166*
Nb–O_{b4}	2.066	2.104	2.072	2.210*	2.045	1.990
W_{eq}–O_c	2.328	2.295	2.308	2.303	2.309	2.378
W_{eq}–O_{b2}	1.946	1.928	2.146*	1.925	1.964	1.932
W_{eq}–O_{b4}	1.903	1.856	1.887	2.122*	2.016	1.935
W_{eq}–O_{b5}	1.967	2.165*	1.935	1.879	1.904	1.954
W_{ax}–O_c	2.353	2.336	2.321	2.332	2.323	2.333
W_{ax}–O_{b1}	1.908	1.907	1.892	1.902	2.127*	1.908
W_{ax}–O_{b2}	1.980	1.987	2.171*	1.992	1.947	1.986
C–O	–	1.453	1.456	1.454	1.456	1.454

* M–O_b (M = Nb, W), in which the metal atoms are connected to methoxy groups.

methoxy groups, are longer, as a result of the interactions between methoxy and the adjacent metal atoms, than the corresponding bonds in the $[Nb_2W_4O_{19}]^{4-}$ anion. The other M–O_b bonds are slightly changed (see Table S1). Going from $[Nb_2W_4O_{19}CH_3]^{3-}$ to $[Nb_2W_4O_{19}]^{4-}$, the Nb–O_b bond lengths are increased by 0.144–0.179 Å and the bond lengths of W–O_b are increased by 0.191–0.219 Å because the ionic radius of Nb^V is smaller than that of W^{VI}. From Table 1, we can see that the C–O bond lengths are unchanged, so we can conclude that different metals do not change the C–O bond distances.

2.2 Stabilities of $[Nb_2W_4O_{19}CH_3]^{3-}$ isomers

The five isomers of $[Nb_2W_4O_{19}CH_3]^{3-}$ have not yet been completely purified. Here, the total bonding energies of the five isomers are analyzed. According to the transition-state method of Ziegler and Rauk [56–58], the molecular bonding energy (E_B) can be described as

$$E_B = E_P + E_O + E_E,$$

where E_P, E_O, and E_E are the Pauli repulsion, orbital mixing term, and electrostatic interaction, respectively. E_E and E_O have stabilizing effects. The Pauli repulsion has a destabilizing effect, caused by the larger energy shift of the antibonding orbital to the bonding orbital.

The bonding energies, as well as the orbital mixings, Pauli repulsions, and electrostatic interactions for the bonding energies of systems B to F in the gas phase are given in Table S2. The calculated total bonding energies (E_B) of the five isomers show the following order: F < B < D < C < E. The bonding energies of system F is the lowest among the five systems since the orbital mixing and electrostatic effects are more favorable in system F. So, system F in the gas phase is the most stable among the five $[Nb_2W_4O_{19}CH_3]^{3-}$ isomers. The E_P of system B is much lower than that of D, so B is more stable than D. Systems C and E are the two chiral isomers. However, the Pauli repulsions of systems C and E are high, and the stabilizing effects are low, making systems C and E less stable than the other three isomers.

The relative energies (E_{Rel}) of the five systems in acetonitrile are shown in Table 2. The solvation energies also stabilize the systems. The results show that the order of the relative stabilities in acetonitrile is as follows: B > F > D > C > E. System B is more stable than system F in acetonitrile. Systems B and F are energetically very stable and are thermodynamically favorable anions. The energies of the two chiral systems C and E are higher than those of the other

Table 2 Relative energies (E_{Rel}) of the five systems and relative energies ($E_{Rel'}$) of the one-electron-reduced $[Nb_2W_4O_{19}CH_3]^{4-}$ isomers in acetonitrile (kJ/mol)

Isomers	B	C	D	E	F
E_{Rel}	0.0	9.54	4.89	12.72	1.88
$E_{Rel'}$	0.0	9.25	1.13	10.00	–1.17

three systems in the gas phase and in solution. It can also be concluded that the methoxy group lying in the equatorial plane is more stable than that lying on the axial surface.

The energy differences among the five systems are small, so PBE and PW91 methods were also used to calculate the energies of the $[Nb_2W_4O_{19}CH_3]^{3-}$ isomers, and the relative energies are collected in Table S3. The relative stabilities of the five isomers obtained using PBE and PW91 are the same as those obtained using the BP86 method.

Calculations were performed for the one-electron-reduced species $[Nb_2W_4O_{19}CH_3]^{4-}$, and the relative energies (E_{Rel}) are listed in Table 2. The order of the stabilities of the one-electron-reduced anions, $[Nb_2W_4O_{19}CH_3]^{4-}$, in acetonitrile is slightly different from that of the fully oxidized anions $[Nb_2W_4O_{19}CH_3]^{3-}$ in acetonitrile; the order is F > B > D > C > E.

2.3 Electronic properties

How does the methoxy group affect the electronic properties of the five isomers? To investigate the effects of the methoxy group on the electronic properties of the polyanions, the frontier molecular orbitals (FMOs) of $[Nb_2W_4O_{19}]^{4-}$ and $[Nb_2W_4O_{19}CH_3]^{3-}$ are compared. The highest occupied molecular orbital (HOMO) in $[Nb_2W_4O_{19}]^{4-}$ formally delocalizes over the bridging oxygen of two niobium atoms and two tungsten atoms, and the bridging oxygen on the axial surface, and the lowest unoccupied molecular orbital (LUMO) delocalizes over the d-shells of the tungsten atoms, with some antibonding participation of oxygen orbitals (Figure 2).

The FMOs of the methoxy-substituted systems are significantly different from those of $[Nb_2W_4O_{19}]^{4-}$. The HOMO of system F delocalizes over the bridging oxygen atoms of the axial surface, and the LUMO delocalizes over the d-shells of the two niobium atoms and axial tungsten atoms, with some antibonding participation of the oxygen orbitals (Figure 2). For systems B and D, the HOMOs delocalize over the eight bridging oxygen atoms of the axial surface. The HOMO in system C mainly delocalizes over the bridging oxygen atoms, which are not located on the surface made by Nb_2, W_2, W_3, and W_4. The HOMO of system E delocalizes over the bridging oxygen atoms, except for the oxygen atoms that are located on the surface made by Nb_1, W_1, W_3, and W_4. The HOMOs in the five isomers therefore formally delocalize over the bridging oxygen atoms, which are distant from the surface containing the methoxy group and four metal atoms. The LUMO delocalizes over the d-shells of four metal atoms close to the methoxy group, and there is some antibonding participation of oxygen orbitals. The FMO distribution suggests that the methoxy group mainly modifies the unoccupied orbitals.

2.4 Redox properties

It is known that redox properties depend on the energy and composition of the LUMO. We now investigate the redox ability of $[Nb_2W_4O_{19}CH_3]^{3-}$ and the reduced center when the cluster is reduced. The LUMO energies and HOMO-LUMO energy gaps of the five isomers are shown in Figure 3. The LUMO energies and the HOMO-LUMO energy gaps of the five isomers are lower than those of $[Nb_2W_4O_{19}]^{4-}$, so electronic transitions between the HOMOs and LUMOs of the $[Nb_2W_4O_{19}CH_3]^{3-}$ isomers are much easier. The LUMO

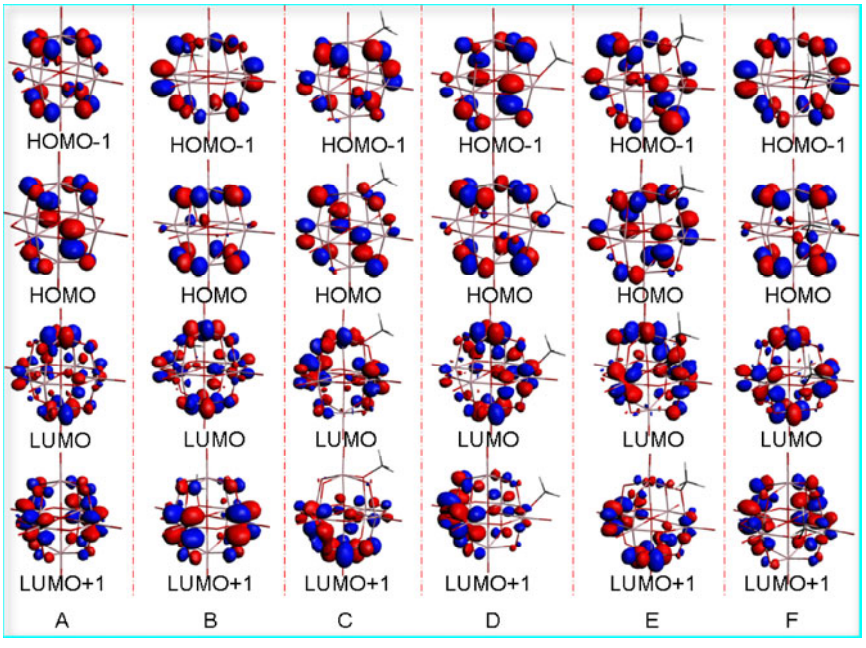

Figure 2 (Color online) Frontier molecular orbitals of $[Nb_2W_4O_{19}]^{4-}$ and $[Nb_2W_4O_{19}CH_3]^{3-}$.

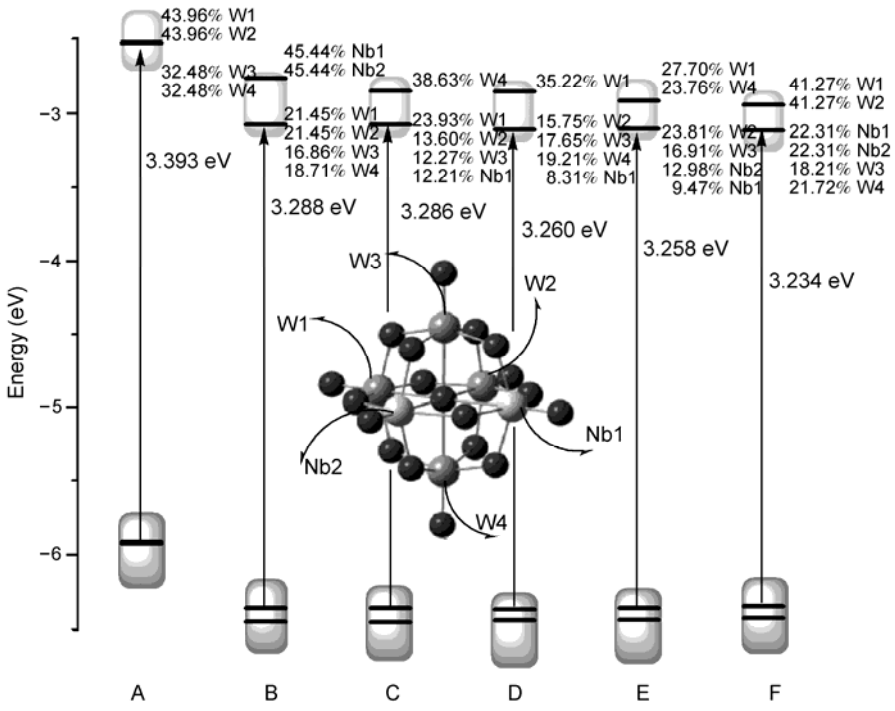

Figure 3 Energy levels of $[Nb_2W_4O_{19}]^{4-}$ and five $[Nb_2W_4O_{19}CH_3]^{3-}$ isomers.

energies of the five isomers are as follows: −3.074 eV (B), −3.070 eV (C), −3.107 eV (D), −3.103 eV (E), and −3.114 eV (F). In particular, system F (methoxy group lying between two niobium atoms) is more likely to obtain one electron than the other four systems are. The redox abilities of systems D and E (methoxy group lying between one niobium atom and one tungsten atom) make this process slightly harder than in system F, but easier than in systems B and C (methoxy group lying between two tungsten atoms). The electron affinities (EAs) were also calculated and described as follows:

$$\text{Oxidized form} + e^- \longrightarrow \text{Reduced form}$$

The EAs of the five isomers are 1.575, 1.579, 1.578, 1.604 and 1.628 eV for B, C, D, E, and F, respectively. So system B is more easily reduced than the other isomers are. The EA values are consistent with the LUMO energies of the studied systems. This demonstrates that the redox properties of the studied isomers are changed by changing the positions of the methoxy groups.

The results suggest that the redox abilities of the five isomers are strong because of the lower LUMO energies of the methoxy-substituted isomers. As shown in Figure 3, the LUMOs of the five isomers are composed of three or four metal atom contributions, and the LUMO of $[Nb_2W_4O_{19}]^{4-}$ is contributed by two tungsten atoms in the equatorial plane. It seems that three or four atoms will accept an extra electron in the five isomers when the cluster is reduced. To investigate the reduced center, calculations were performed on the reduced species $[Nb_2W_4O_{19}CH_3]^{4-}$. The spin densities of the $[Nb_2W_4O_{19}]^{5-}$ anion are −0.0060, 0.0283, and 0.1314 for Nb, W_{ax}, and W_{eq}, respectively. It can be seen that the extra electron in the monoreduced $[Nb_2W_4O_{19}]^{5-}$ localizes on the tungsten atoms in the equatorial plane. The spin densities of $[Nb_2W_4O_{19}CH_3]^{4-}$ are presented in the Table 3. The results suggest that the extra electron in the monoreduced $[Nb_2W_4O_{19}CH_3]^{4-}$ localizes on the tungsten atoms.

The four tungsten atoms of system B have comparable spin densities, so the four tungsten atoms will accept one electron in system B. For systems C and E, one-electron-reduction will occur on two tungsten atoms. For systems D and F, there is only one tungsten atom with high spin-density. Obviously, the methoxy group also changes the reduced centers of the five systems.

According to the literature [59,60], electron-transfer reactions account for the behaviors of the studied systems. The electronic excitation energies and corresponding oscillator strengths for the $[Nb_2W_4O_{19}]^{5-}$ anion and $[Nb_2W_4O_{19}CH_3]^{4-}$ isomers are presented in Table 4. It is evident that the excitation energies of systems B, C, and E are similar to that of system A. The excitation energy of system D is larger

Table 3 Spin density (α–β) of five $[Nb_2W_4O_{19}CH_3]^{4-}$ isomers

Isomers	B	C	D	E	F
Nb1	−0.0196	0.0392	0.0188	0.0288	0.0647
Nb2	−0.0196	−0.0146	−0.0100	0.0452	0.0647
W1	0.0816	0.1579	−0.0263	−0.0256	−0.0124
W2	0.0816	0.1157	0.1682	0.1261	−0.0124
W3	0.1157	0.0802	0.0986	0.1987	0.0892
W4	0.0795	−0.0227	0.0887	−0.0095	0.1689

Table 4 Calculated electronic excitation energies (nm), corresponding oscillator strengths, and the corresponding dominant molecular orbital (MO) transitions of $[Nb_2W_4O_{19}]^{4-}$ and the five $[Nb_2W_4O_{19}CH_3]^{3-}$ isomers

	Excitation energies	Oscillator strengths	Dominant MO transitions
A	299	0.014	HOMO-2→LUMO+1 (58.08%) HOMO→LUMO (28.81%)
B	300	0.019	HOMO-2→LUMO (91.78%)
C	303	0.007	HOMO-3→LUMO (51.45%) HOMO-1→LUMO (19.94%) HOMO-4→LUMO (13.98%)
D	307	0.017	HOMO-1→LUMO (63.58%) HOMO-2→LUMO (19.69%)
E	302	0.009	HOMO→LUMO+1 (54.50%) HOMO-1→LUMO+1 (12.91%)
F	290	0.020	HOMO-2→LUMO (67.70%) HOMO-1→LUMO+1 (14.42%) HOMO-3→LUMO+1 (12.01%)

than that of A by 8 nm, and the electronic excitation energy of system F is 290 nm, which is smaller than that of A. The order of the oscillator strengths for the systems is F ≈ B ≈ D > A > E ≈ C. So, the position of the methoxy group affects the excitation energies of the studied isomers.

3 Conclusions

The effects of methoxy groups on the electronic properties and stabilities of POMs were investigated using DFT calculations. The results can be summarized in four principal conclusions. (1) The M–O_b (M = Nb, W) bond lengths in the five $[Nb_2W_4O_{19}CH_3]^{3-}$ isomers, in which the metal atoms are connected with the methoxy group, are longer than those in $[Nb_2W_4O_{19}]^{4-}$. (2) In the gas phase, the total bonding energies (E_B) of the $[Nb_2W_4O_{19}CH_3]^{3-}$ isomers lead to the following order of stability: F > B > D >C > E. In acetonitrile, system B is more stable than system F. (3) The methoxy group modifies the FMOs of the five isomers. The LUMOs of the fully oxidized $[Nb_2W_4O_{19}CH_3]^{3-}$ isomers are different from that of $[Nb_2W_4O_{19}]^{4-}$, and they localize on the four metal atoms that are close to the methoxy group. The HOMOs in the five isomers formally delocalize over the bridging oxygen atoms, which are distant from the surface containing the methoxy group and the four metal atoms. (4) The LUMO energies in the five isomers are lower than that of $[Nb_2W_4O_{19}]^{4-}$, and electronic transitions between the HOMOs and LUMOs of the methoxy-functionalized POM $[Nb_2W_4O_{19}CH_3]^{3-}$ are much easier than that in $[Nb_2W_4O_{19}]^{4-}$. The additional electrons in the one-electron-reduced species, the $[Nb_2W_4O_{19}CH_3]^{4-}$ isomers, mainly delocalize over the tungsten atoms.

This work was supported by the National Natural Science foundation of China (20971020, 21073030 and 21131001), the Doctoral Fund of the Ministry of Education of China (20100043120007), and the Science and Technology Development Planning of Jilin Province (20100104).

1 Pope M T, Müller A. Polyoxometalate Chemistry: An old field with new dimensions in several disciplines. Angew Chem Int Ed Eng, 1991, 30: 34–48
2 Muller A, Kogerler P, Kuhlmann C. A variety of combinatorially linkable units as disposition: [dagger] from a giant icosahedral Keplerate to multi-functional metal-oxide based network structures. Chem Commun, 1999, 15: 1347–1358
3 Pope M T. Heteropoly and Isopoly Oxometalates. New York: Springer-Verlag, 1983. 1–180
4 López X, Bo C, Poblet J M. Electronic properties of polyoxometalates: Electron and proton affinity of mixed-dddenda Keggin and Wells-Dawson anions. J Am Chem Soc, 2002, 124: 12574–12582
5 Kozhevnikov I V. Catalysis by heteropoly acids and multicomponent polyoxometalates in Liquid-Phase reactions. Chem Rev, 1998, 98: 171–198
6 Judd D A, Nettles J H, Nevins N, et al. Polyoxometalate HIV-1 protease inhibitors. A new mode of protease inhibition. J Am Chem Soc, 2001, 123: 886–897
7 Aguey-Zinsou K F, Bernhardt P V, Kappler U, et al. Direct electrochemistry of a bacterial sulfite dehydrogenase. J Am Chem Soc, 2003, 125: 530–535
8 Ogliaro F, de Visser S P, Cohen S, et al. Searching for the second oxidant in the catalytic cycle of cytochrome P450: A theoretical investigation of the iron(III)-hydroperoxo species and its epoxidation pathways. J Am Chem Soc, 2002, 124: 2806–2817
9 Zhang T R, Feng W, Lu R, et al. Thermochromic organoaminomodified silica composite films containing phosphomolybdic acid. J Solid State Chem, 2002, 166: 259–263
10 Lindqvist I. Ark.Kemi. Stockholm: Almqvist och Wiksell, 1950
11 Tytko K H, Baethe G, Hirschfeld E R, et al. Über die gleichgewichte in wäßrigen polymolybdatlösungen neuauswertung der potentiometrischen meßdaten von SASAKI und SILLÉN. Z Anorg Allg Chem, 1983, 503: 43–66
12 Dabbabi M, Boyer M, Launay J P, et al. Propriétés électrochimiques de polyanions mixtes de composition $Nb_nW_{6-n}O_{19}^{(2+n)-}$(*n*=0, 1, 2, 3 et 4). J Electroanal Chem Inter Electrochem, 1977, 76: 153–164
13 Maestre J M, Sarasa J P, Bo C, et al. *Ab initio* study of the relative basicity of the external oxygen sites in $M_2W_4O_{19}^{4-}$ (M = Nb and V). Inorg Chem, 1998, 37: 3071–3077
14 Day V W, Klemperer W G, Schwartz C. Synthesis, characterization, and interconversion of the niobotungstic acid $Nb_2W_4O_{19}H^{3-}$ and its anhydride and alkyl/silyl esters. J Am Chem Soc, 1987, 109: 6030–6044
15 Koch W, Holthausen M C. A Chemist's Guide to Density Functional Theory. Weinheim: Wiley-VCH, 2001
16 Duclusaud H, Borshch S A. Iron-molybdenum electron delocalization in substituted Keggin polyoxoanions. Inorg Chem, 1999, 38: 3489–3493
17 Maestre J M, Lopez X, Bo C, et al. Electronic and magnetic properties of α-Keggin anions: A DFT study of $[XM_{12}O_{40}]^{n-}$, (M = W, Mo; X = Al^{III}, Si^{IV}, P^{V}, Fe^{III}, Co^{II}, Co^{III}) and $[SiM_{11}VO_{40}]^{m-}$ (M = Mo and W). J Am Chem Soc, 2001, 123: 3749–3758
18 Yan L K, Su Z M, Tan K, et al. Electronic properties of Strandberg anions: A DFT study of $[X_2Mo_5O_{23}]^{n-}$, (X = P^{V}, S^{VI}, As^{V}, Se^{VI}), and $[(RP)_2Mo_5O_{21}]^{4-}$ (R = H, CH_3, C_2H_5). Int J Quantum Chem, 2005, 105: 37–42
19 Guan W, Yang G C, Yan L K, et al. How do the different defect structures and element substitutions affect the nonlinear optical properties of lacunary Keggin polyoxometalates? A DFT study. Eur J

Inorg Chem, 2006, 2006: 4179–4183
20 Yan L K, Dou Z, Guan W, et al. A DFT study on the electronic and redox properties of $[PW_{11}O_{39}(ReN)]^{n-}$($n$ = 3, 4, 5) and $[PW_{11}O_{39}(OsN)]^{2-}$. Eur J Inorg Chem, 2006, 2006: 5126–5129
21 Guan W, Yang G, Liu C, et al. Reversible redox-switchable second-order optical nonlinearity in polyoxometalate: A quantum chemical study of $[PW_{11}O_{39}(ReN)]^{n-}$ (n = 3–7). Inorg Chem, 2008, 47: 5245–5252
22 Guan W, Liu C, Song P, et al. Quantum chemical study of redox-switchable second-order optical nonlinearity in Keggin-type organoimido derivative $[PW_{11}O_{39}(ReNC_6H_5)]^{n-}$($n$=2–4). Theor Chim Acta, 2009, 122: 265–273
23 Rohmer M M, Devémy J, Wiest R, et al. *Ab initio* modeling of the endohedral reactivity of polyoxometallates: 1. Host-guest interactions in $[RCN(V_{12}O_{32})^{4-}]$ (R = H, CH_3, C_6H_5). J Am Chem Soc, 1996, 118: 13007–13014
24 Maestre J M, Poblet J M, Bo C, et al. Electronic structure of the highly reduced polyoxoanion $[PMo_{12}O_{40}(VO)_2]^{5-}$: A DFT study. Inorg Chem, 1998, 37: 3444–3446
25 Rohmer M M, Bénard M, Blaudeau J P, et al. From Lindqvist and Keggin ions to electronically inverse hosts: *Ab initio* modelling of the structure and reactivity of polyoxometalates. Coord Chem Rev, 1998, 178-180(Part 2): 1019–1049
26 López X, Maestre J M, Bo C, et al. Electronic properties of polyoxometalates: A DFT study of α/β-$[XM_{12}O_{40}]^{n-}$ relative stability (M = W, Mo and X a main group element). J Am Chem Soc, 2001, 123: 9571–9576
27 Bridgeman A J, Cavigliasso G. Electronic structure of the α and β isomers of $[Mo_8O_{26}]^{4-}$. Inorg Chem, 2002, 41: 3500–3507
28 Maestre J M, Lopez X, Bo C, et al. A DFT study of the electronic spectrum of the α-Keggin anion $[Co^{II}W_{12}O_{40}]^{6-}$. Inorg Chem, 2002, 41: 1883–1888
29 Bridgeman A J, Cavigliasso G. Computational analysis of Mo and W oxoanions through bond order and bonding energy approaches. J Phys Chem A, 2003, 107: 4568–4577
30 Poblet J M, Lopez X, Bo C. *Ab initio* and DFT modelling of complex materials: Towards the understanding of electronic and magnetic properties of polyoxometalates. Chem Soc Rev, 2003, 32: 297–308
31 Ziegler T. Approximate density functional theory as a practical tool in molecular energetics and dynamics. Chem Rev, 1991, 91: 651–667
32 Rosa A, Baerends E J. Metal-macrocycle interaction in phthalocyanines: Density functional calculations of ground and excited states. Inorg Chem, 1994, 33: 584–595
33 Gracia J, Poblet J M, Autschbach J, et al. Density-functional calculation of the ^{183}W and ^{17}O NMR chemical shifts for large polyoxotungstates. Eur J Inorg Chem, 2006, 2006: 1139–1148
34 Hu Y H, Ruckenstein E. Endohedral chemistry of C60-based fullerene cages. J Am Chem Soc, 2005, 127: 11277–11282
35 Korchowiec J, Korchowiec B, Priebe W, et al. DFT study on the selectivity of complexation of metal cations with a dioxadithia crown ether ligand. J Phys Chem A, 2008, 112: 13633–13640
36 Lee T B, McKee M L. Endohedral hydrogen exchange reactions in C60 ($n$$H_2$@C60, n=1–5): Comparison of recent methods in a high-pressure cooker. J Am Chem Soc, 2008, 130: 17610–17619
37 Datta A. Role of metal ions (M = Li^+, Na^+, and K^+) and pore sizes (Crown-4, Crown-5, and Crown-6) on linear and nonlinear optical properties: New materials for optical birefringence. J Phys Chem C, 2009, 113: 3339–3344
38 Mbomekallé M, López X, Poblet J M, et al. Influence of the heteroatom size on the redox potentials of selected polyoxoanions. Inorg Chem, 2010, 49: 7001–7006
39 Fonseca Guerra C, Snijders J G, te Velde G, et al. Towards an order-N DFT method. Theor Chim Acta, 1998, 99: 391–403
40 te Velde G, Bickelhaupt F M, Baerends E J, et al. Chemistry with ADF. J Comput Chem, 2001, 22: 931–967
41 ADF2009. 01, SCM. Theoretical Chemistry. Amsterdam: Vrije Universiteit, http://www. scm. com
42 Vosko S H, Wilk L, Nusair M. Accurate spin-dependent electron liquid correlation energies for local spin density calculations: A critical analysis. Can J Phys, 1980, 58: 1200–1211
43 Becke A D. Density-functional exchange-energy approximation with correct asymptotic behavior. Phys Rev A, 1988, 38: 3098
44 Perdew J P. Density-functional approximation for the correlation energy of the inhomogeneous electron gas. Phys Rev B, 1986, 33: 8822
45 Yan L, Jin M, Song P, et al. Electronic properties of unprecedented bridging organoimido-substituted hexamolybdate: New insights from density functional theory study. J Phys Chem B, 2010, 114: 3754–3758
46 Chang C. Regular two-component pauli-like effective hamiltonians in dirac theory. Phys Scr, 1986, 34: 394
47 van Lenthe E, Baerends E J, Snijders J G. Relativistic regular two-component Hamiltonians. J Chem Phys, 1993, 99: 4597–4610
48 van Lenthe E, Baerends E J, Snijders J G. Relativistic total energy using regular approximations. J Chem Phys, 1994, 101: 9783–9792
49 van Lenthe E, van Leeuwen R, Baerends E J, et al. Relativistic regular two-component Hamiltonians. Int J Quantum Chem, 1996, 57: 281–293
50 Zerfos P, Zhong G, Cheng J, et al. DIRAC: A software-based wireless router system. 2003, 230–244
51 Andzelm J, Kolmel C, Klamt A. Incorporation of solvent effects into density functional calculations of molecular energies and geometries. J Chem Phys, 1995, 103: 9312–9320
52 Klamt A. Conductor-like screening model for real solvents: A new approach to the quantitative calculation of solvation phenomena. J Phys Chem, 1995, 99: 2224–2235
53 López X, Weinstock I A, Bo C, et al. Structural evolution in polyoxometalates: A DFT study of dimerization processes in Lindqvist and Keggin cluster anions. Inorg Chem, 2006, 45: 6467–6473
54 Romo S, Fernández J A, Maestre J M, et al. Density functional theory and *ab initio* study of electronic and electrochemistry properties of the tetranuclear sandwich complex $[Fe^{III}_4(H_2O)_2(PW_9O_{34})_2]^{6-}$. Inorg Chem, 2007, 46: 4022–4027
55 Schipper P R T, Gritsenko O V, van Gisbergen S J A, et al. Molecular calculations of excitation energies and (hyper)polarizabilities with a statistical average of orbital model exchange-correlation potentials. J Chem Phys, 2000, 112: 1344–1352
56 Ziegler T, Rauk A. On the calculation of bonding energies by the Hartree Fock Slater method. Theor Chim Acta, 1977, 46: 1–10
57 Ziegler T, Rauk A. A theoretical study of the ethylene-metal bond in complexes between copper(1+), silver(1+), gold(1+), platinum(0) or platinum(2+) and ethylene, based on the Hartree-Fock-Slater transition-state method. Inorg Chem, 1979, 18: 1558–1565
58 Ziegler T, Rauk A. Carbon monoxide, carbon monosulfide, molecular nitrogen, phosphorus trifluoride, and methyl isocyanide as .sigma. donors and .pi. acceptors. A theoretical study by the Hartree-Fock-Slater transition-state method. Inorg Chem, 1979, 18: 1755–1759
59 Zhao G J, Liu J Y, Zhou L C, et al. Site-selective photoinducedelectron transfer from alcoholic solvents to the chromophore facilitated by hydrogen bonding: A new fluorescence quenching mechanism. J Phys Chem B, 2007, 111: 8940–8945
60 Zhao G J, Han K L. Site-Specific solvation of the photoexcited protochlorophyllide a in methanol: Formation of the hydrogen-bonded intermediate state induced by hydrogen-bond strengthening. Biophys J, 2008, 94: 38–46